ANALYTICAL SOLUTIONS TO CONSTRAINED HYPERSONIC FLIGHT TRAJECTORIES

Ping Lu*

Iowa State University

Ames, IA 50011

Abstract

The flight trajectory of aerospace vehicles subject to a class of path constraints is considered. The constrained dynamics is shown to be a natural two-time-scale system. Asymptotic analytical solutions are obtained. Problems of trajectory optimization and guidance can be dramatically simplified with these solutions. Applications in trajectory design for an aerospace plane strongly support the theoretical development.

1. Introduction

In many flight control and trajectory optimization problems, certain portions of the trajectory are required to follow some state space constraints dictated by operational or safety considerations. Nowadays almost all realistic atmospheric flight problems are numerically intensive. Solutions to these constrained problems are thus in the form of numerical data. Analytic expressions of the constrained trajectory as explicit functions of time, if available, are the dream of a trajectory designer. They provide an efficient means to evaluate the trajectory, and often lead to a better understanding of the trajectory. In turn, tasks such as trajectory optimization, control and guidance can be significantly simplified. In some cases approximate analytical solutions may be possible because of the additional relationships due to the constraints. Gilbert *et al* present an enlightening treatment of a coasting arc observed in the optimal trajectory of a ground-based interceptor[1]. But in general, no systematic approach exists to obtain analytical solutions to the constrained system which is often nonlinear in nature. This paper extends the approach in Ref. 1

* Assistant Professor, Department of Aerospace Engineering and Engineering Mechanics, Member AIAA.

to more general flight problems. For an important class of constrained flight problems which are described in Section 2.1, the dynamics is shown to be a two-time-scale system. Approximate analytical asymptotic solutions are obtained. Successful applications in the optimal ascent and hypersonic cruising trajectory analyses for an aerospace plane are presented. Comparison of the approximate solutions with numerically generated solutions shows excellent agreement.

2. Theoretical Development

2.1 Problem Formulation

Consider the point-mass model for a vehicle flying in a fixed great circle plane over a nonrotating spherical earth. Define the dimensionless variables

$$h = \frac{r - r_o}{r_o}, \quad v = \frac{V}{\sqrt{g_o r_o}}, \quad \tau = \frac{t - t_o}{\sqrt{r_o/g_o}} \tag{1}$$

where r is the distance from the center of the earth to the vehicle; V the speed; t the current time. r_o and g_o are the radius and gravitational acceleration, respectively, at the starting time t_o. The dynamics is given by

$$h' = v \sin\gamma \tag{2}$$

$$\theta' = \frac{v \cos\gamma}{1+h} \tag{3}$$

$$v' = \frac{T - D}{m g_o} - \frac{sin\gamma}{(1+h)^2} \tag{4}$$

$$\gamma' = \frac{L}{m g_o v} + (\frac{v}{1+h} - \frac{1}{v(1+h)^2}) \cos\gamma \tag{5}$$

The prime in Eqs. (2)–(5) denotes the differentiation with respect to τ. An algebraic constraint is imposed on the trajectory

$$C(v, \rho(h)) = 0 \tag{6}$$

In the above equations γ stands for the flight path angle, θ the down range polar angle, T the thrust, L and D the aerodynamic lift and drag, respectively. ρ in Eq. (6) represents the atmospheric density.

Assumptions:

(i) The dependence of the magnitude of the thrust T on altitude, if any, is exclusively through atmospheric density or dynamic pressure.

(ii) The atmospheric density is an exponential function of altitude

$$\rho = \rho_o e^{-\beta h} \triangleq \rho_o \bar{\rho}(h) \tag{7}$$

where $\beta = r_0/h_s$ with h_s being the scale height.

(iii) The constraint contains ρ explicitly, i.e., $\partial C/\partial \rho \neq 0$. At the starting point $C(v(t_o), \rho_o) = 0$. $\partial C/\partial v \neq 0$ for $t \geq t_o$. Then by the implicit function theorem v can be regarded as a function of ρ

$$v = f(\bar{\rho}(h)) \tag{8}$$

(iv) The set of feasible controls is not empty. We define here a pair of controls $[T(t), \alpha(t)]$ to be feasible if the solutions of Eqs. (2)–(5) satisfy Eq. (6), and $0 \leq T(t) \leq T_{max}$ and $\alpha_{min} \leq \alpha(t) \leq \alpha_{max}$, where T_{max} is the maximum available thrust (which may be altitude dependent), and α_{min} and α_{max} are the lower and upper bound of angle of attack, respectively.

(v) $|\gamma|$ is small along all feasible trajectories.

Assumption (i) is valid for many flight scenarios and both airbreathing and rocket propulsion systems. Note that (i) includes pure coasting case when $T = 0$. Assumptions (ii) is easily justified. Assumption (iii) specifies the class of constraints under consideration. Many important physical constraints in hypersonic flight are in this class. Assumption (v) is often satisfied during constrained flight.

2.2 Asymptotic Solutions

In the following analysis, we assume that the vehicle is flying along a feasible trajectory. We proceed by first differentiating (8) once

$$v' = \frac{\partial f}{\partial \bar{\rho}} \frac{\partial \bar{\rho}}{\partial h} h' = -\beta f_{\bar{\rho}} \bar{\rho} v \sin\gamma \tag{9}$$

By (4) and (9),

$$-\beta f_{\bar{\rho}} \bar{\rho} v \sin\gamma = \frac{T - D}{m g_o} - \frac{sin\gamma}{(1+h)^2} \tag{10}$$

There are two controls for the vehicle, T and α. Either one of the controls can be pre-programmed or determined by some type of performance optimization. The other control is then determined from Eq. (10) to satisfy the constraint, provided that the resulting control pair is in the set of feasible controls defined by Assumption (iv). It is understood that the following discussions apply to such a case. Once T and α are determined, we can define the lift-to-drag ratio

$$\eta = \frac{L}{D} \tag{11}$$

and the thrust-to-drag ratio

$$\kappa = \frac{T}{D} \tag{12}$$

η is primarily a function of Mach number for given α, and κ a function of Mach number and atmospheric density for given throttle setting. Next, neglect the gravity component in the v' equation for small γ

$$v' = \frac{T - D}{mg_o} = \frac{(\kappa - 1)D}{mg_o} \tag{13}$$

Consider the flight path angle equation (5). We note that typically $h << 1$ for atmospheric flight, and γ is assumed to be small. Using $\cos\gamma \approx 1$, $1 + h \approx 1$ and $L = \eta D$ in (5), we have

$$\gamma' = \frac{1}{v}(\frac{\eta D}{mg_o} - 1 + v^2) \tag{14}$$

Assume that $\kappa \neq 1$. Replacing D in (14) by (13) yields

$$\gamma' = \frac{1}{v}(\frac{v'\eta}{\kappa - 1} - 1 + v^2) \tag{15}$$

Noticing $v = f(\bar{\rho})$, we substitute v' in (15) by Eq. (9) to obtain

$$\gamma' = (-\frac{\beta f_{\bar{\rho}} \bar{\rho} \eta}{\kappa - 1}\gamma - \frac{1}{f} + f) \tag{16}$$

To explore the solution, we define new scaled variables

$$\bar{h} = \beta h, \quad \bar{\gamma} = \beta\gamma \tag{17}$$

From Eqs. (2) and (16) the equations for the two new variables are

$$\bar{h}' = v\bar{\gamma} \tag{18}$$

$$\varepsilon\bar{\gamma}' = (-\frac{f_{\bar{\rho}}\bar{\rho}\eta}{\kappa - 1}\bar{\gamma} - \frac{1}{f} + f) \tag{19}$$

where $\varepsilon = 1/\beta = h_s/r_o$. For the earth, ε is on the order of 10^{-3}. By Assumption (i) κ is a function of $\bar{h}$ through the density. The right hand side of Eq. (19) is independent of ε. Therefore, we see that equations (18)–(19) constitute a natural two-time-scale system. By the standard singular perturbation theory[2], the sufficient condition that $f_{\bar{\rho}}\eta/(\kappa - 1) > 0$ guarantees that the system has an attracting asymptotic solution to which the solution of the system will quickly converge. The zeroth-order outer solution is obtained by setting the right hand of Eq. (19) equal to zero

$$\bar{\gamma} = e^{\bar{h}}\frac{(f - f^{-1})}{f_{\bar{\rho}}}\frac{(\kappa - 1)}{\eta} \tag{20}$$

where $\bar{\rho} = e^{-\bar{h}}$ has been used. Substituting (20) and $v = f$ into (18) gives

$$\frac{d\bar{h}}{d\tau} = -P\frac{1 - f^2}{\bar{\rho}f_{\bar{\rho}}} \tag{21}$$

where

$$P = \frac{\kappa - 1}{\eta} \tag{22}$$

Noticing that $df = -\bar{\rho}f_{\bar{\rho}}d\bar{h}$, we have

$$\frac{df}{1 - f^2} = Pd\tau \tag{23}$$

which, upon integration, yields

$$v = f = \frac{e^{2z(\tau)} + Q}{e^{2z(\tau)} - Q} \tag{24}$$

In (24) Q and $z(\tau)$ are defined by

$$Q = \frac{v_o - 1}{v_o + 1} \tag{25}$$

$$z(\tau) = \int_0^\tau P(\sigma)d\sigma \tag{26}$$

Discussions

(1) Equation (20) provides an approximate closed-form solution for γ along the constrained trajectory. This formula can be very useful for guidance purposes. The accuracy is to the degree of $\sin\gamma \approx \gamma$ and $1 + h \approx 1$. Notice that f and $f_{\bar{p}}$ can be evaluated from C [Eq. (6)] via the implicit function theorem.

(2) The solution (20) is the zeroth-order outer solution. In general, the initial condition on γ will not be satisfied. In dimensionless time τ, this solution will only be accurate outside the initial boundary layer of thickness on the order of ε, which corresponds to a few seconds in real time.

(3) When $T = D$ (or $\kappa = 1$) at some isolated points, a singularity arises at those points. Formulas (20) and (24) then represent the outer solutions in the intervals separated by those points. There is a small neigborhood around each of those points where the the outer solutions are inaccurate. When $T \equiv D$, it can be shown from Eqs. (2) and (4) that

$$h = \frac{1}{\sqrt{(v^2 - v_0^2)/2 + 1}} - 1$$

If we substitute above equation into Eq (6), Eq. (6) becomes an algebraic equation in v. It is clear that the constrained trajectory can only have a constant speed which is a root of Eq. (6). This in turn implies that the altitude can only be constant. Thus $\gamma \equiv 0$. Letting $\kappa \equiv 1$ and $z(\tau) \equiv 0$ in Eqs. (20), (21) and (24), we arrive at $\gamma \equiv 0$, $h \equiv h_0 = 0$ and $v \equiv v_0$, which verifies that the above formulas are still valid in this case.

(4) Interestingly, the variation in v is not explicitly dependent on the form of the constraint (6) according to Eq. (24). A similar formula is obtained in Ref. 1 for a specific constraint. But here we show that this is a general result for the class of constraints under consideration. Another nice feature of the above formulas is that there is no explicit dependence on the mass m which is time-varying for $T \neq 0$. The only inconvenience in the explicit formulas (24) is the function $z(\tau)$. In some case z may take a simple form as an example will demonstrate later. For more general situations often an estimate of the average value of P, say, $\bar{P}$, may be used in (26). Then,

$$z(\tau) \approx \bar{P}\tau \tag{27}$$

If necessary, $\bar{P}$ can always be estimated without much difficulty from numerical simulation of the accurate trajectory. The errors introduced by this approximation are limited because any errors in h and γ are about one thousand times smaller than those in $\bar{h}$ and $\bar{\gamma}$, owing to the scaling effect of Eq. (17). In the post-run data analysis, having to estimate $\bar{P}$ in the analytic representations is much better than to sort through the numerical data. With this simplification the explicit solution for θ is found to be

$$\theta' \approx v \Longrightarrow \theta - \theta_o = \bar{P} \ln(\frac{e^{2\bar{P}\tau} - Q}{1 - Q}) - \tau \tag{28}$$

(5) Up to this point, the discussion is general in the sense that no specific forms of C in Eq. (6) have been assumed, as long as Assumption (iii) is valid. $\bar{h}$ is an implicit function of time through (6) and (24). If, however, h can be solved explicitly in terms of v from Eq. (6), then $\bar{h}$ can be expressed as a function of time. $\bar{\gamma}$ can thus be obtained as an explicit function of time through (20).

Let us consider two types of constraints that will be used in the next section.

<u>Case 1</u>

$$C = v\bar{\rho}^p - C_p = 0, \quad C_p > 0 \text{ and } p \text{ any nonzero real number} \tag{29}$$

Hence

$$v = f = C_p \bar{\rho}^{-p} = C_p e^{p\bar{h}}, \quad \bar{h} = \frac{1}{p} \ln(f/C_p) \tag{30}$$

The solutions for $\bar{h}$ and $\bar{\gamma}$ are

$$\bar{h}(\tau) = \frac{1}{p} \ln(\frac{e^{2z(\tau)} + Q}{C_p(e^{2z(\tau)} - Q)}) \tag{31}$$

$$\bar{\gamma}(\tau) = \frac{P}{p}((\frac{e^{2z(\tau)} - Q}{e^{2z(\tau)} + Q})^2 - 1) \tag{32}$$

<u>Case 2</u>

C is a function of v and ρ, and v can be expressed as

$$v = f = (A + B\bar{\rho}^m)^n \tag{33}$$

where A, B, m and n are all nonzero real numbers such that $f(e^{-\bar{h}}) > 0$. **Case 1** can actually be included in (33) if we allow A to be zero. Nevertheless, we list the formulas here seperately for the convenience of later reference.

$$\bar{\rho}^m = \frac{(e^{2z(\tau)} + Q)^{1/n} - A(e^{2z(\tau)} - Q)^{1/n}}{B(e^{2z(\tau)} - Q)^{1/n}} \triangleq g(\tau) \tag{34}$$

$$\bar{\gamma}(\tau) = P\frac{(A + Bg(\tau))^n - (A + Bg(\tau))^{-n}}{nmB(A + Bg(\tau))^{n-1}g(\tau)} \tag{35}$$

$$\bar{h}(\tau) = -\frac{1}{m}\ln g(\tau) \tag{36}$$

We conclude this section by stressing that the point at t_0 ($\tau = 0$) does not have to be the point where the trajectory just enters the constraint (6). It can be a midway point on the constraint. By letting τ have negative values, the expressions for $v(\tau)$, $\gamma(\tau)$, $h(\tau)$ and $\theta(\tau)$ are valid for the portion of the trajectory before t_0. This feature can be very useful in characterizing a family of constrained trajectories which enter the same constraint at different points.

3. Applications in Trajectory Analysis for an Aerospace Plane

3.1 Optimal Ascent to Orbit

An aerospace plane is a hypersonic vehicle that has single-stage-to-orbit (SSTO) capability. The primary propulsion comes from airbreathing engines. There has been active study of the fuel-optimal ascent trajectory for the aerospace plane[3-6]. It is found that a typical optimal trajectory will sequentially climb on two operational constraints

$$q = \frac{1}{2}\rho V^2 = q_{max} \tag{36}$$

$$\dot{Q} = K\sqrt{\rho}V^3 = \dot{Q}_{max} \tag{37}$$

The first one is a dynamic pressure constraint and the second a convective heating rate constraint. In conformity with Eq. (29), the two constraints can be rewritten as, respectively,

$$v\bar{\rho}^{0.5} = ve^{-0.5\bar{h}} = C_q \tag{38}$$

$$v\bar{\rho}^{1/6} = ve^{-\bar{h}/6} = C_{\dot{Q}} \tag{39}$$

where

$$C_q = \sqrt{2q_{max}/\rho_o g_o r_o}, \quad C_{\dot{Q}} = (\dot{Q}_{max}/K g_o r_o \sqrt{\rho_o g_o r_o})^{1/3} \tag{40}$$

A generic aerospace plane model[7] is used. The thrust of the airbreathing propulsion system is modeled by

$$T = C_T q \tag{41}$$

where the thrust coefficient C_T is a function of dynamic pressure, Mach number and the throttle, controlled by the fuel equivalence ratio. Hence the model satisfies Assumption (i). For the best fuel efficiency the equivalence ratio is set at unity. Assumption (v) has been verified[6].

A typical optimal ascent trajectory for the aerospace plane is shown in Fig. 1. After a quick initial climb-out, the trajectory enters the q-constraint boundary and rides on it until the $\dot{Q}$-constraint becomes active. After flying on the $\dot{Q}$-constraint awhile the aerospace plane finally pulls up at an appropriate point and ascends to orbit. When the aerospace plane is flying on the constraint (36), the complete trajectory is characterized by

$$v = \frac{e^{2\bar{P}\tau} + Q}{e^{2\bar{P}\tau} - Q} \tag{42}$$

$$\bar{h} = 2\ln\left(\frac{e^{2\bar{P}\tau} + Q}{C_q(e^{2\bar{P}\tau} - Q)}\right) \tag{43}$$

$$\bar{\gamma} = 2\bar{P}\left(\left(\frac{e^{2\bar{P}\tau} - Q}{e^{2\bar{P}\tau} + Q}\right)^2 - 1\right) \tag{44}$$

$$\theta = \theta_o + \bar{P}\ln\left(\frac{e^{2\bar{P}\tau} - Q}{1 - Q}\right) - \tau \tag{45}$$

The approximation of (27) has been used in the above equations. Similar formulas with $p = 1/6$ in Eqs. (31) and (32) describe the motion analytically after the aerospace plane leaves the constraint (36) and enters the constraint (37). When $q_{max} = 95{,}660$ N/m^2 (2,000 psf) and $\dot{Q}_{max} = 800$ W/cm^2, we choose $\bar{P} = 0.9$ and $\bar{P} = 1.2$ for the q-constraint and $\dot{Q}$-constraint respectively, based on the results in Ref. 6. Figures 2 and 3 compare the the analytic solutions with the numerical solutions obtained in Ref. 6. We see that both the altitude and flight path angle histories match quite well.

The trajectory optimization for the aerospace plane stands as a very challenging problem because of the highly data-driven model and stringent flight path constraints. Since the dominant portion of the optimal ascent trajectory is on the constraints (36) and (37)[3-6], formulas (42)–(45) and their counterparts for the constraint (37) provide a simple yet accurate representation of $60\% - 80\%$ of the trajectory. The trajectory optimization problem can be considerably simplified by only numerically investigating the rest of the trajectory.

It is also worth pointing out that Eq. (32) indicates a nonzero flight path angle along the constraints (36) and (37). Applications of the standard energy state approximation and zeroth order time-scale decomposition technique to the unconstrained trajectory lead to the reduced solution $\gamma = 0$[3,5]. The presence of the two constraints obviously has altered the structure of the reduced solution, as suggested by Moerder *et al* [5] from a different perspective. Equations (18) and (19) imply that on the constraint boundary only the flight path angle dynamics should be considered "fast" instead of both altitude and flight path angle dynamics being considered "fast". This phenomenon is more evident in the next problem.

3.2 Hypersonic Cruise

During the early flight tests of the aerospace plane and some other conceivable missions, a considerable portion of the trajectory will be hypersonic cruise inside the atmosphere[8]. A natural design of the cruising trajectory is a nearly horizontal path with lift-to-drag ratio nearly maximized. To this end, we would want the cruising trajectory to follow a constraint

$$C(v,\rho,h) = \frac{\rho_o r_o S C_L^*}{2m_o}\bar{\rho}v^2 + (\frac{v^2}{1+h} - \frac{1}{(1+h)^2}) = 0 \qquad (46)$$

where S is the reference area of the vehicle and C_L^* the lift coefficient corresponding to α^*, the angle of attack at which the lift-to-drag ratio L/D is maximized. Constraint (46) is the result of letting $\gamma = 0$ and $L = L^*$ in the right hand side of the γ' equation (5) and setting γ' to zero. It should be noted that during the flight the actual γ will not be exactly zero since the velocity is varying thus α will be slightly different from α^*. However, the

flight path angle γ will be near zero and α will be near α^* if (46) is followed. Solving v in terms of ρ and h produces

$$v = \sqrt{\frac{1}{(1+h)(1+G(1+h)\bar{\rho})}} \tag{47}$$

with the constant G being defined as

$$G = \frac{\rho_o r_o S C_L^*}{2m_o} \tag{48}$$

Because of the constraint, γ is expected to be small, and so is h. Therefore,

$$v = f(\bar{\rho}) = \sqrt{\frac{1}{1+G\bar{\rho}}} \tag{49}$$

We first investigate the trajectory numerically. To fly the vehicle, the throttle setting is fixed at a constant by specifying a fuel equivalence ratio. The aerodynamic control, α, required to follow the constraint (47) is obtained by solving the equation $C' = 0$. Then the α is used in Eqs.(4) and (5) to generate the actual flight trajectory. For computation, we have chosen the following data:

$$\text{equivalence ratio} = 0.5, \quad \text{initial altitude} = 40 \text{ km}, \quad m_o = 100{,}000 \text{ kg}, \quad \gamma_o = 0$$

The initial Mach number is 14.63 determined by (47). Figure 4 shows the variations of γ and α for the first 10 seconds of the flight obtained through numerical integration. Both histories exhibit an unmistakable transient period of 3–4 seconds. After this period γ and α settle down in a steady state with α approaching α^* which is 3.93° for our case. This asymptotic (as $t \to \infty$) behavior is found to be present regardless of the starting altitude and throttle setting, which renders strong support to the theory developed in Section 2.2, Eq. (19) in particular. Then we turn to the analytical asymptotic solution of the trajectory which is given by Eqs. (35) and (36) with $A = 1$, $B = G$, $n = -1/2$ and $m = 1$:

$$\bar{\gamma} = 2P\left(\frac{e^{2z(\tau)} - Q}{e^{2z(\tau)} + Q}\right)^2 \tag{50}$$

$$\bar{h} = \ln\left(\frac{G(e^{2z(\tau)} + Q)^2}{-4Qe^{2z(\tau)}}\right) \tag{51}$$

The function $z(\tau)$ can be calculated as follows. Since $\alpha \approx \alpha^*$ except for the short initial period,

$$\eta = \frac{L}{D} \approx (\frac{L}{D})_{max} \tag{52}$$

$$\kappa = \frac{T}{D} \approx \frac{C_T}{SC_D^*} \tag{53}$$

C_T is treated as a constant for the given equivalence ratio and the range of altitude and Mach number variations. Then,

$$P = \frac{\kappa - 1}{\eta} = \text{constant}, \quad z(\tau) = P\tau \tag{54}$$

The complete trajectory is designed in the following way: The climbing trajectory from takeoff to the beginning of the cruise is numerically found by the inverse dynamics technique presented in Ref. 6. This results in a fuel-optimal trajectory subject to inequality constraints $q \leq q_{max}$ and $\dot{Q} \leq \dot{Q}_{max}$, equality constraints $h_f = 40$ km, $\gamma_f = 0°$ and v_f =Mach 14.63. The cruising trajectory then is analytically modeled by Eqs. (24), (50) and (51). Figures 5 demonstrates the complete trajectory. The asymptotic solution shows an excellent agreement with the cruising trajectory obtained by numerical integration. Figure 6 compares the asymptotic and numerical solutions for γ along the cruising part of the trajectory. Except for the a few initial seconds, the asymptotic solution again is very close the the true solution. The Mach number increases from 14.63 to 15.29 at the end of the ten-minute cruise. It should be noted that the choice of the cruising altitude and throttle setting only influences the magnitudes of the h, v and γ. The characteristics of the trajectory remain the same.

Conclusions

The flight trajectory of aerospace vehicles subject to a class of path constraints has been studied. The analysis reveals that under some fairly general conditions the altitude dynamics and flight path angle dynamics constitute a natural two-time-scale system: the flight path angle dynamics is fast and the altitude dynamics slow. The approximate asymptotic solution for the flight path angle is given as a function of the altitude from which the velocity can be expressed as an explicit function of time, regardless of the specific forms of the constraints. If the altitude can be solved in terms of the velocity from the constraint,

both the altitude and the flight path angle have analytical expressions as functions of time. Applications in trajectory analysis for an aerospace plane are presented. The challenging problem of ascent trajectory optimization for the aerospace plane can be significantly simplified by using these analytical formulas. The technique is also used to design a hypersonic cruising trajectory for the aerospace plane. The results strongly support the theory and the analytical solutions are in excellent agreement with the numerical results.

Acknowledgments

This research was supported by NASA Langley Research Center under Contract No. NAG-1-1255 for which Dr. Daniel D. Moerder is the the technical monitor. This work has also benefited greatly from the inspiring discussions with Professor E. G. Gilbert at the time when the author was with the University of Michigan.

References

[1] Gilbert, E. G., Howe, R. M., Lu, P. and Vinh, N. X., "Optimal Aeroassisted Intercept Trajectories At Hyperbolic Speeds", *AIAA Journal of Guidance, Control, and Dynamics*, Vol. 14, No. 1, Jan.–Feb., 1991, pp. 123–131.

[2] O'Malley, R. E., Jr., "On Nonlinear Singularly Perturbed Initial Value Problems", *SIAM Review*, Vol. 30,No. 2, 1988, pp. 193–212.

[3] Corban, J. E., Calise, A. J, and Flandro, G. A., "Rapid Near-Optimal Aerospace Plane Trajectory Generation and Guidance", *AIAA Journal of Guidance, Control, and Dynamics*, Vol. 14, No. 6, November–December, 1991, pp. 1181–1190.

[4] Van Buren, M. A., and Mease, K. D., "Aerospace Plane Guidance Using Time-Scale Decomposition and Feedback Linearization", *AIAA Journal of Guidance, Control, and Dynamics*, Vol. 15, No. 5, Sept.–Oct., 1992, pp. 1166–1174.

[5] Moerder, D. D., Pamadi, B., and Dutton, K., "Constrained Energy State Suboptimal Control Analysis of a Winged-Cone Aero-Space Plane Concept", AIAA-91-5053, Third International Aerospace Planes Conference, Orlando, FL, 3–5, December, 1991.

[6] Lu, P., "An Inverse Dynamics Approach to Trajectory Optimization and Guidance for an Aerospace Plane", *Proceedings of AIAA Guidance, Navigation, and Control Conference*, Hillton Head, SC, August 10–12, 1992.

[7] Shaughnessy, J. D., Pinckey, S. Z., McMinn J. D., Cruz, C. I., and Kelley M-L., "Hypersonic Vehicle Simulation Model: Winged-Cone Configuration", NASA TM 102610, November 1990.

[8] "JPO Studying Flight Test Issues In Early Phases of X-30 Program", *Aviation Week & Space Technology*, October 29, 1990, pp. 46–47.

List of Captions

Fig. 1 Typical optimal ascent trajectory for an aerospace plane

Fig. 2 Comparison of asymptotic and numerical altitude histories

Fig. 3 Comparison of asymptotic and numerical flight path angle histories

Fig. 4 Asymptotic behaviors of flight path angle γ and angle of attach α

Fig. 5 Climbing+cruisng trajectory: altitude vs. down range

Fig. 6 Comparison of asymptotic and numerical flight path angle histories along the cruising trajectory

Fig. 1

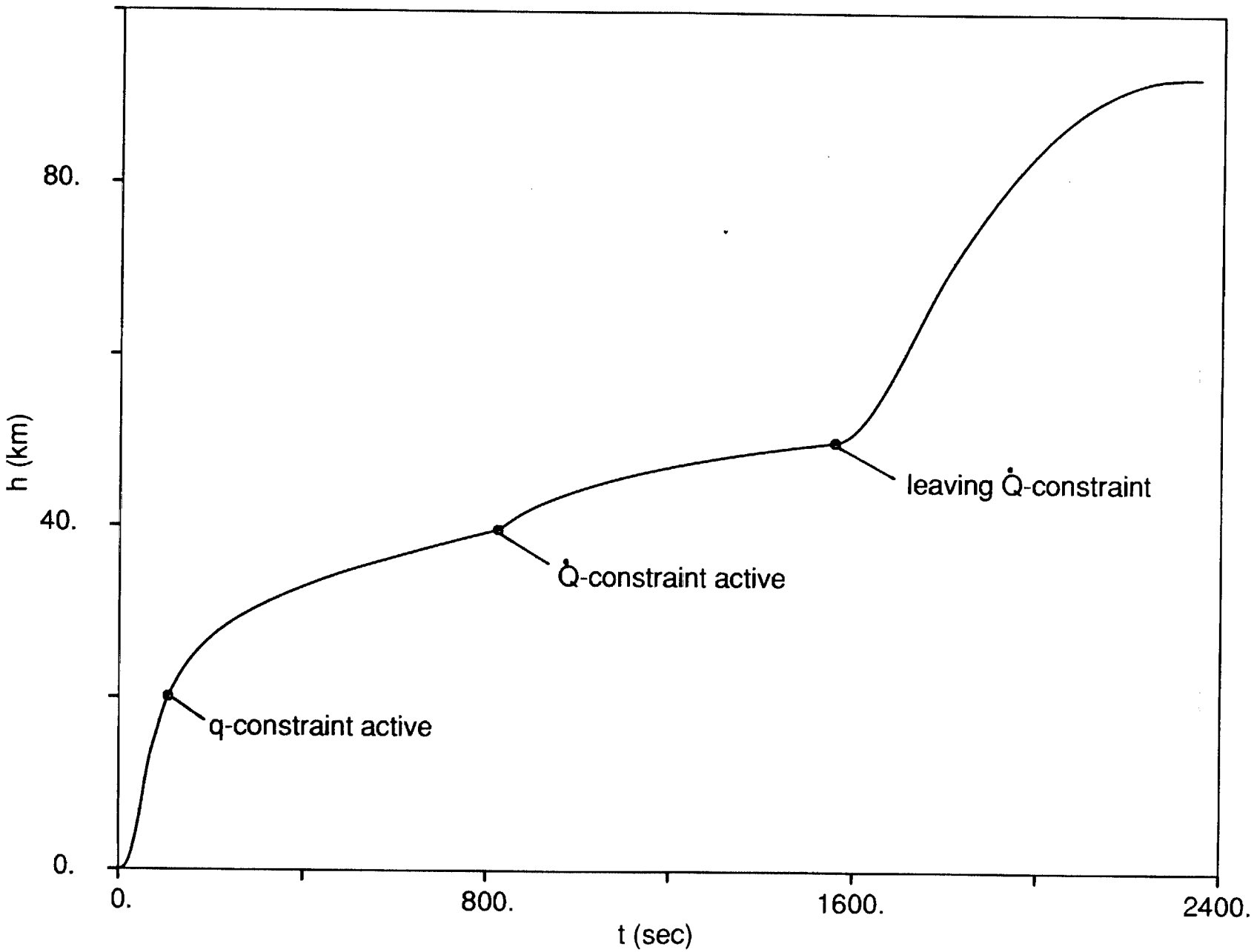
80.
40.
0.
h (km)
0.
800.
1600.
2400.
t (sec)
q-constraint active
Q̇-constraint active
leaving Q̇-constraint

Fig. 2

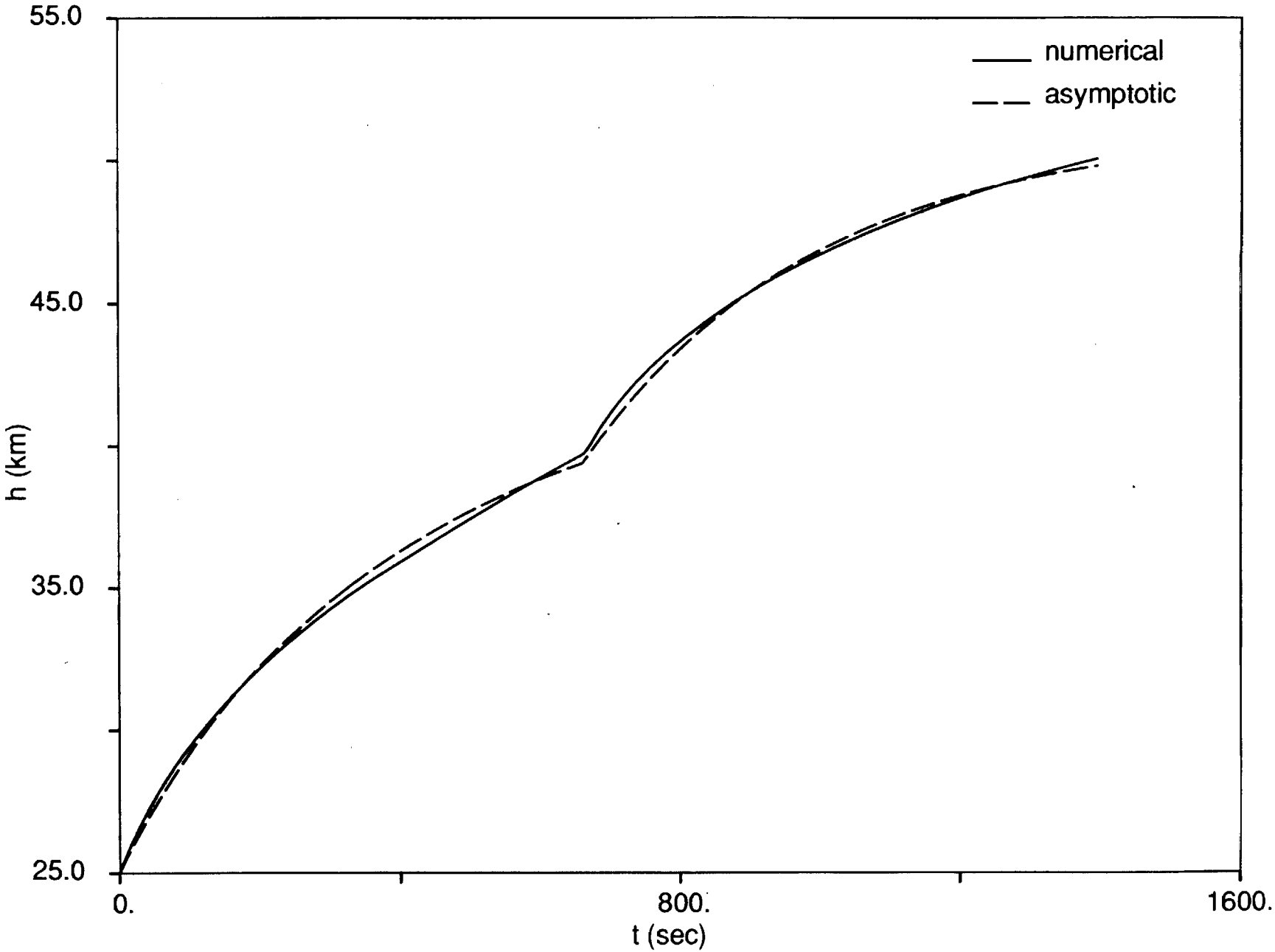

Fig. 3

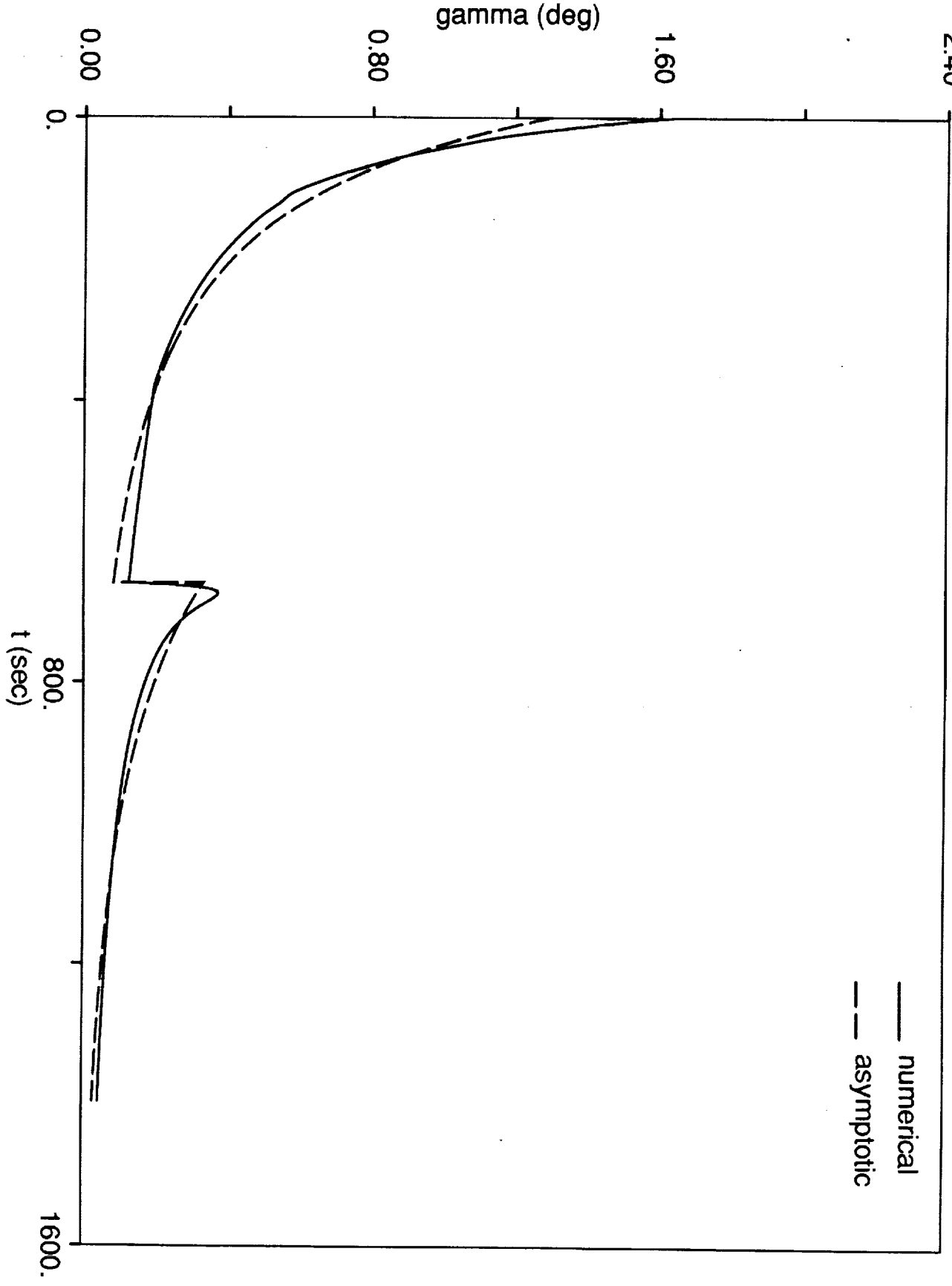
gamma (deg)
0.00
0.80
1.60
2.40
0.
800.
1600.
t (sec)
numerical
asymptotic

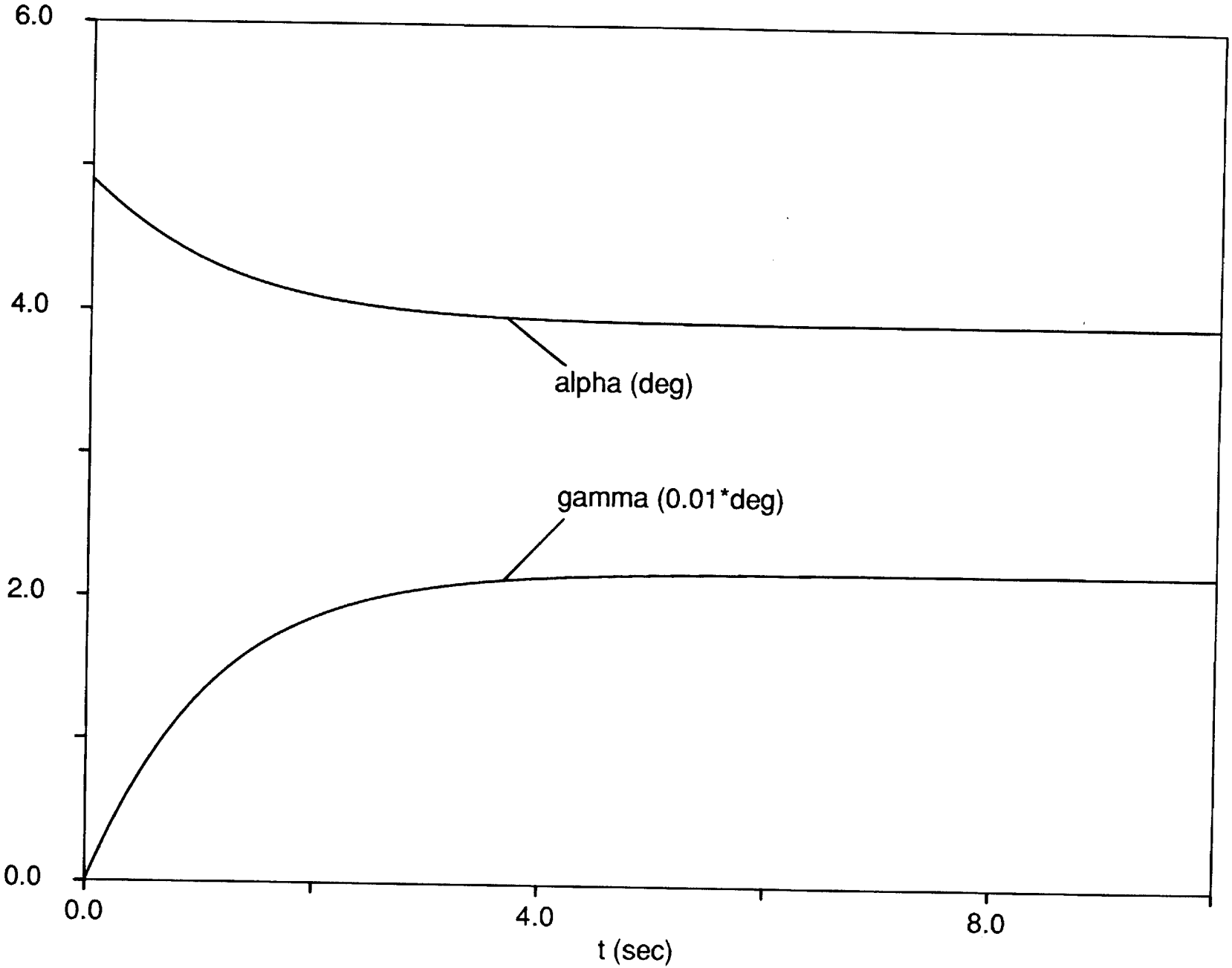
6.0
4.0
2.0
0.0
alpha (deg)
gamma (0.01*deg)
0.0
4.0
8.0
t (sec)

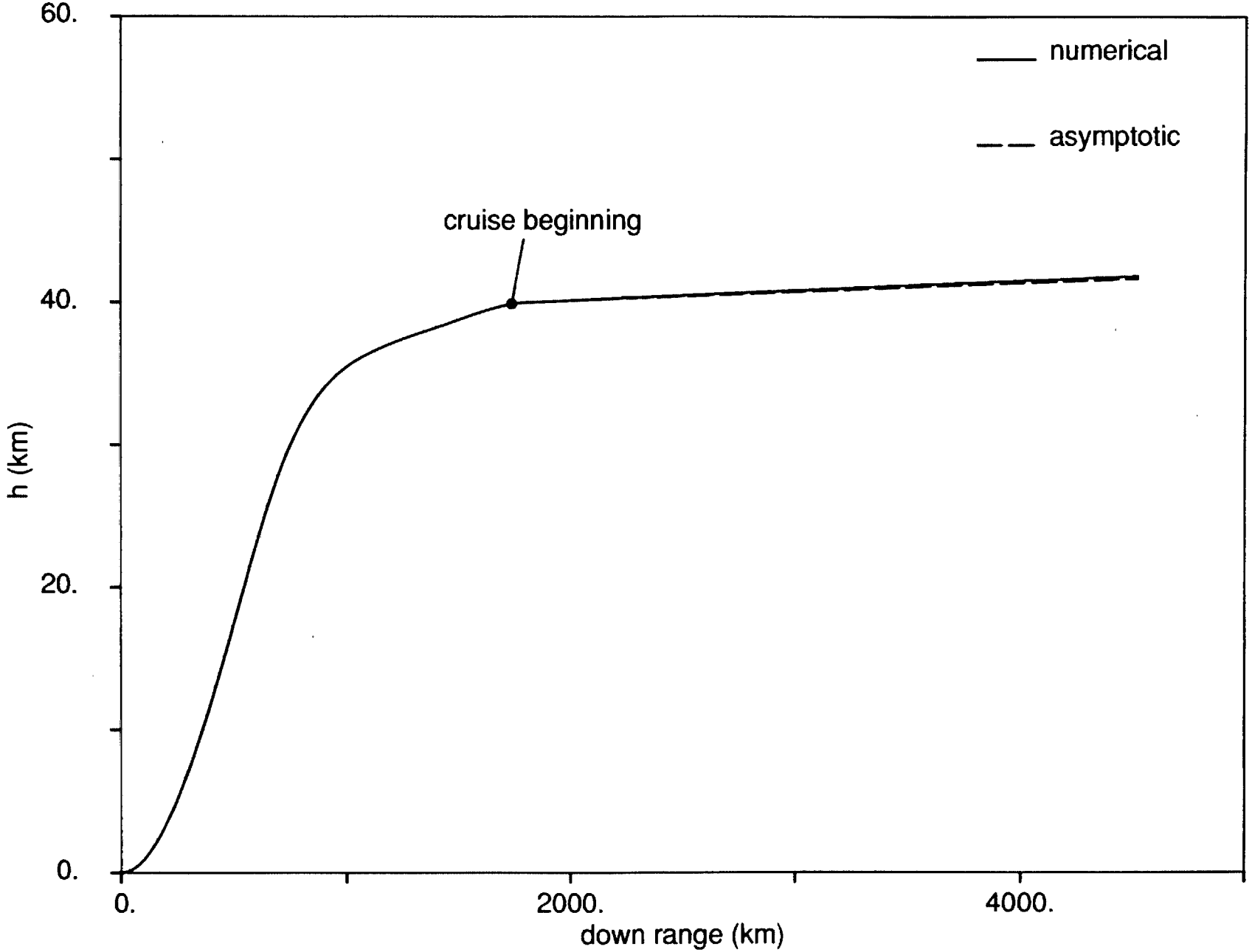
60.
40.
20.
0.
h (km)
0.
2000.
4000.
down range (km)
numerical
asymptotic
cruise beginning

Fig. 6

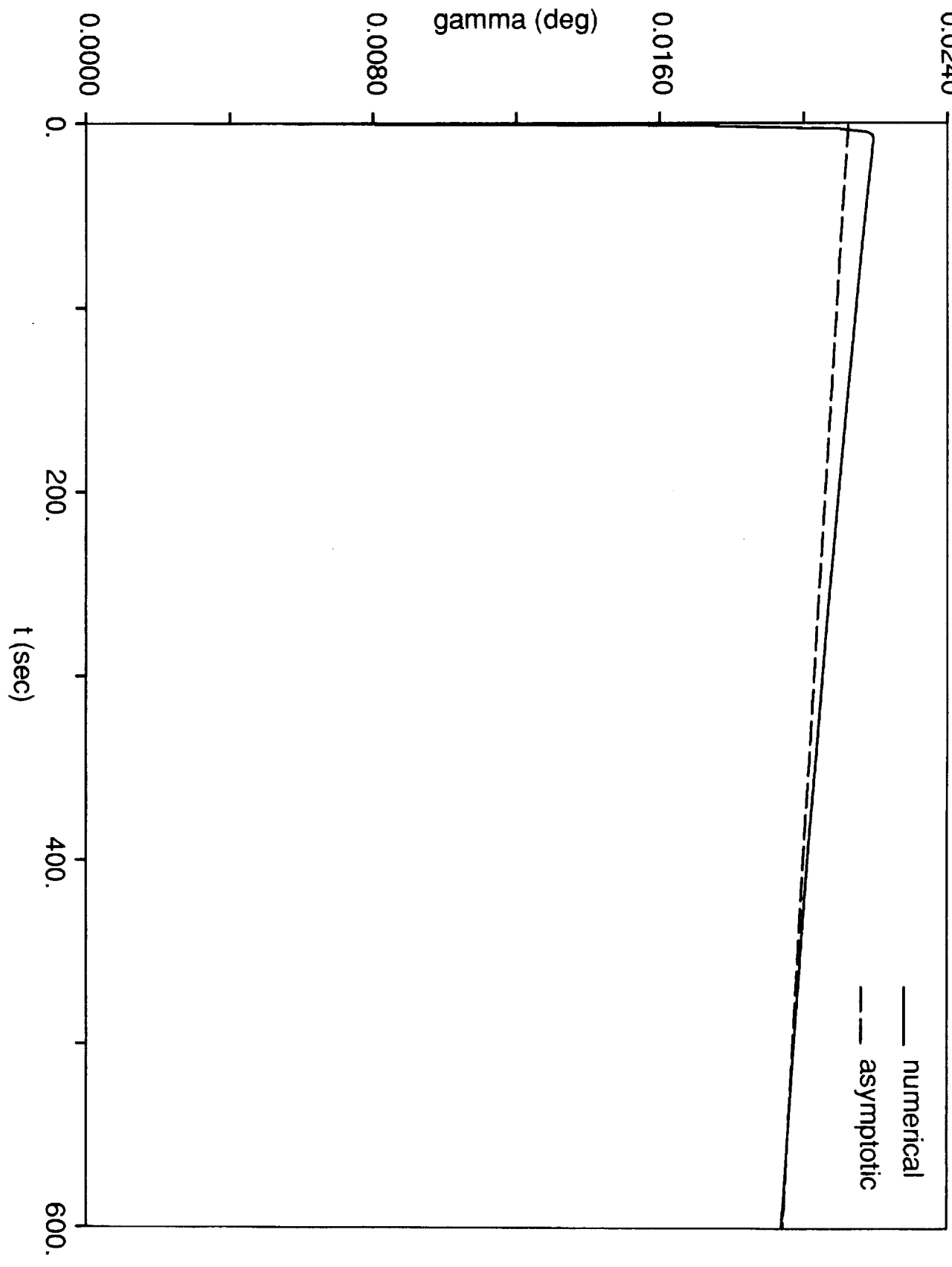
gamma (deg)
0.0000
0.0080
0.0160
0.0240
0.
200.
400.
600.
t (sec)
numerical
asymptotic